Available online at www.sciencedirect.com
SCIENCE DIRECT®
Surface Science 519 (2002) 173–184
SURFACE SCIENCE
www.elsevier.com/locate/susc

Adsorption and photodissociation of 4-haloanilines on GaN(0 0 0 1)

V.M. Bermudez *

Naval Research Laboratory, 4555 Overlook Ave., SW Washington, DC 20375-5347, USA

Received 20 May 2002; accepted for publication 3 July 2002

Abstract

The adsorption of 4-chloro- and 4-iodoaniline on the GaN(0 0 0 1)-(1 × 1) surface, and the subsequent effects of exposure to near- or vacuum-ultraviolet radiation, have been studied. Both species adsorb via the molecular NH_2 group, with the phenyl ring intact, as does aniline itself. Like aniline, both are very reactive with the clean surface, requiring only a small dose to reach saturation coverage. 4-Iodoaniline is photochemically active as an adsorbate on GaN. Ultraviolet radiation promotes dissociation of the molecular C–I bond, leading to the transfer of I to available Ga sites on the GaN surface. The process then terminates when all such sites are filled. Dissociation of the C–I bond does not appear to involve photoexcited carriers from the substrate and is, instead, suggested to occur through direct excitation of the adsorbate. The photochemical activity of 4-chloroaniline adsorbed on GaN is at present uncertain, but it appears to be relatively inert.

Keywords: Ab initio quantum chemical methods and calculations; Auger electron spectroscopy; Electron energy loss spectroscopy (EELS); Photoelectron spectroscopy; Photochemistry; Gallium nitride; Aromatics; Halogens

1. Introduction

The rapidly developing interest in nanotechnology has stimulated research into the patterned growth of organic films on semiconductor surfaces. One approach is to construct patterned organic layers "from the bottom up". Here one first "functionalizes" the surface by chemisorbing an appropriate reagent [1,2] then builds a structure by photochemical reaction with a second species, stimulated by ultraviolet (UV) radiation through a mask [3]. With a suitable choice of adsorbates, it would be possible to build a particular chemical functionality into the patterned structure [4].

It has recently been shown [5,6] that organic amines chemisorb readily, via the molecular N atom, on the Ga-polar GaN(0 0 0 1) surface with the molecular N–C and C–C bonds remaining intact. Hence a bifunctional amine, one with a second sterically accessible and easily photolyzable functional group, might enable patterning of organic layers on GaN(0 0 0 1). The wide band gap of hexagonal GaN ($E_g = 3.4$ eV, vs. 1.14 eV for Si) offers advantages in the design of hybrid organic/semiconductor structures. For example, in

* Tel.: +1-202-767-6728; fax: +1-202-404-4071.
E-mail address: bermudez@estd.nrl.navy.mil (V.M. Bermudez).

0039-6028/02/$ - see front matter
PII: S0039-6028(02)02146-5

electro-optic devices visible access to the interface can be obtained through the substrate. The wider band gap also allows more flexibility in selecting organic adsorbates such that the lowest unoccupied molecular orbital (LUMO) lies near the substrate conduction band minimum (CBM). This alignment of energy levels will be a factor in charge transport across the interface. Organic layers may also be useful in modifying metal/GaN interfaces, as shown for Au/GaAs [7], which would be particularly important in making low-resistance contacts to p-type GaN.

In the present work, we advance in this direction through a study of the chemisorption of 4-chloro- and 4-iodoaniline on the GaN(0 0 0 1) surface and the effects of subsequent exposure to UV radiation. A prerequisite for understanding the photochemical effects is a study of the electronic spectra of these species as adsorbates on GaN, and the results obtained here help in interpreting and reinforcing previous work on simpler amines. The principal techniques used are UV photoemission, electron energy loss, X-ray-excited Auger electron and X-ray photoemission spectroscopies (UPS, ELS, XAES and XPS, respectively), supported by ab initio quantum-chemical calculations.

4-Chloroaniline exhibits a rich and complex near-UV photochemistry [8–12]. However, the dominant mechanism involves heterolytic cleaving of the C–Cl bond to form a cationic carbene and a Cl^- ion. 4-Fluoroaniline behaves similarly [8]. This requires a polar solvent and is not expected to proceed easily in the gas phase or, perhaps, in the chemisorbed state. Little is known about the photochemistry of 4-bromo- and 4-iodoaniline; however, homolytic C–I cleaving to yield a phenylamine radical and an I atom is thought to occur for the latter [13].

2. Experimental details

Details concerning the sample preparation and experimental techniques are given elsewhere [5,6]. The same n- and p-type samples used previously were employed here. The data shown were all obtained for the p-GaN sample, and no significant differences were noted for the n-type material. 4-Chloroaniline (nominally 98% pure) was obtained commercially [1] as a powder with a room-temperature vapor pressure of ~30 mTorr [14]. The raw material was purified by recrystallization from an ethanol solution [15]. 4-Iodoaniline (nominally 98% pure) was obtained commercially [2] in the form of a powder with a vapor pressure of ~3–4 mTorr, as determined using the capacitance manometer on the dosing manifold (see below), and used without further purification. For either compound, the purity was checked by comparing an infrared (IR) transmission spectrum of a solution in CCl_4 to standard reference data [16].

Exposures were performed using a doser [17] with a 100 μm pinhole. The large-diameter pinhole facilitated work with the low-vapor-pressure 4-haloanilines. In either case the powder was stored in a glass bulb, mounted on the doser inlet manifold, which was shielded from ambient light. Adsorbed H_2O was removed by evacuation for several hours with a liquid-N_2-trapped diffusion pump. The vapor pressures were too low for meaningful residual gas analysis via the quadrupole mass spectrometer in the ultra-high vacuum (UHV) chamber. However, no contamination other than a trace of oxygen (see below) was observed in XPS after exposure to either species followed by several hours of data collection.

Most photochemical treatments were done using a 200 Watt high-pressure Hg-arc through a CaF_2 UHV window having a nominal UV transmission limit at ~130 nm. A circular aperture in front of the window masked the outer edge from the UV radiation, which can degrade the AgCl cement used to make the seal [18]. Before entering the chamber the light passed through a 5 cm cell of deionized H_2O, with UV-grade quartz windows, and a UV-grade quartz lens. The H_2O cell reduced sample heating by absorbing radiation at $\lambda > 900$ nm. The Hg-arc emits a series of intense lines, superimposed on a weak continuum, from the near-UV into the near-IR [19]. The total power

[1] Lancaster Synthesis, Inc., P.O. Box 1000, Windham, NH 03087-9977, USA.

[2] Aldrich Chemical Co., Inc., 1001 West Saint Paul Ave. Milwaukee, WI 53233, USA.

incident on the sample, at energies above the GaN absorption edge, was measured using a pyroelectric power meter. For a representative wavelength of ~300 nm, the power density of 0.20 W/cm^2 corresponds to a flux of 2.9×10^{17} photons/cm^2 s.

Some use was also made of a Tanaka-type capillary discharge in H_2 [20,21] which produces a weak continuum from the near-UV to ~165 nm and a more intense line spectrum in the 165–100 nm (7.5–12.4 eV) range. No filtering was used, and no sample heating occurred with this source. A flux at the sample of $\sim 3.4 \times 10^{14}$ photons/cm^2 s was estimated by measuring the total photocurrent from a clean Au foil, grounded through an electrometer, and applying the (photoelectron yield)/(absorbed photon) [22] at 7.5 eV and the reflectance calculated from the Au optical constants [23]. For both sources (Hg-arc and H_2 discharge) the radiation was incident nominally along the surface normal.

The fluxes from the He DC discharge used in UPS and the Mg X-ray source used for XPS and XAES were determined from the Au photocurrent, as described above, and the yield values at $h\nu = 21.2$ [21] and 1253.6 eV [24]. The results are about 1.4×10^9 and 7.0×10^{12} photons/cm^2 s, respectively, for the UPS and XPS sources. These are several orders of magnitude less than the flux from the Hg-arc, and it will be shown below that the UPS and XPS sources cause little or no damage to the adsorbed molecules during the course of data collection.

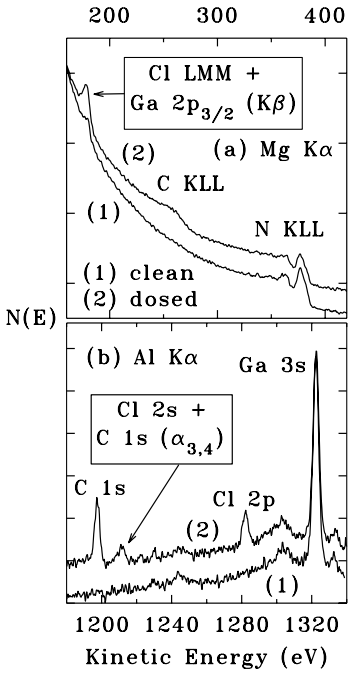

Fig. 1. (a) Partial Mg Kα ($h\nu = 1253.6$ eV) spectra for a GaN(0 0 0 1) surface before and after a saturation dose of 4-chloroaniline. (b) Partial spectra for Al Kα ($h\nu = 1486.6$ eV) excitation, which places features of interest above the range of the strong Ga LMM spectrum. The relative intensities of (a) and (b) are not quantitative, and various XAES and XPS features are labelled. All spectra were recorded with an instrumental resolution of ~1.6 eV and smoothed with a fifth-order, nine-point polynomial. The Ga 3s plasmon loss satellite at ~1300 eV and the Ga 3s Kα$_{3,4}$ satellite at ~1330 eV are not labelled. The very weak feature at ~1245 eV is the Ga $L_1M_{45}M_{45}$ XAES peak. Note the different energy scales for (a) and (b).

3. Results and discussion

3.1. XAES and XPS

Figs. 1 and 2 show typical XAES and XPS data after saturation doses of 4-chloro- and 4-iodoaniline, respectively. A study of the dose dependence was not done, but typical doses were $\sim 9.0 \times 10^{15}$ (2.3×10^{15}) molecules/cm^2 for 4-chloro- (4-iodo-) aniline. These were more than sufficient to saturate the surface in that further exposure resulted in little or no further adsorption. The C KLL/N KLL relative intensity for 4-iodoaniline (not shown) was similar to that in Fig. 1. The saturation coverage of C (viz. phenyl rings) was estimated for 4-chloroaniline using the C KLL and N KLL spectra after background removal and integration [5]. The result was $\Theta_{ph} = 0.29$ monolayers (MLs), where 1 ML is defined as one phenyl ring per surface lattice site. This is essentially identical to the value obtained previously [5] for the adsorption of aniline on this surface. [3] A similar analysis for

[3] The coverage analysis in Ref. [5] employs the (C 1s)/(N 1s) relative photoionization cross-section for Mg Kα$_{1,2}$ excitation with no correction for additional ionization by bremsstrahlung, etc. However, these corrections [25] are nearly the same for C KLL and N KLL XAES and essentially cancel in estimates of relative intensity.

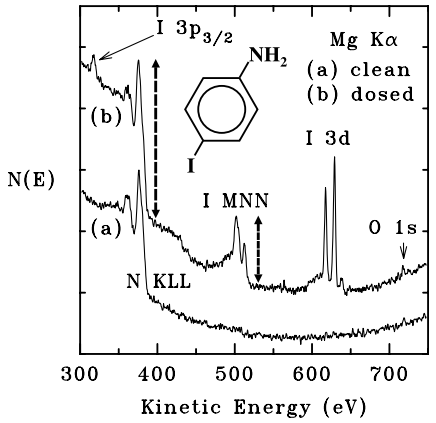

Fig. 2. Mg Kα spectra for (a) clean GaN(0 0 0 1) and (b) after adsorption of 4-iodoaniline. The raw data have been smoothed with a fifth-order, nine-point polynomial. Various Auger and XPS features are labelled. The dashed vertical arrows indicate the N KLL and I MNN Auger peak heights used to quantify changes in I coverage with surface treatment. The instrumental resolution is ~1.6 eV. The inset shows the structure of 4-iodoaniline. To clarify notation, the #1 C is bonded to the NH_2 and the #4 to the halogen.

4-iodoaniline was complicated by the presence of the I $3p_{3/2}$ peak between the C KLL and N KLL spectra (Figs. 1 and 2). As before [5,6], the Al Kα-excited C 1s XPS did not exhibit any resolvable fine-structure, due in part to the large linewidth. The N 1s XPS of the adsorbate is not readily accessible with either Mg or Al Kα excitation because of poor surface sensitivity and interference from Ga LMM XAES features.

The Cl XAES and XPS features, in comparison to those for I, are weaker and more seriously affected by overlap with other structure. Thus the main Cl LMM peak nearly coincides with the Mg Kβ satellite of the strong Mg $K\alpha_{1,2}$-excited Ga $2p_{3/2}$ at ~132 eV, and the Cl 2s falls amidst the Al $K\alpha_{3,4}$ satellites of the Al $K\alpha_{1,2}$-excited C 1s. The relative heights of the Cl 2p and Ga 3s peaks in Fig. 1 were used to assess changes in the Cl coverage with UV exposure. Little or no effect was seen; however, due to the low intensity of the Cl 2p peak, small changes would be difficult to detect reliably.

The relative heights of the main I MNN and N KLL peaks (Fig. 2) were used to assess changes in I coverage. The height of the broad I MNN peak is less likely to be affected by small changes in shape or width, if any, than is that of the narrow I 3d structure. However, trends in the I 3d intensity followed those in the I MNN. After a 5 min Hg-arc exposure (not shown) the (I MNN)/(N KLL) peak-height ratio decreased slightly, to 82 ± 8% of the initial value (average of four runs). The sample temperature rose to about 77 °C during exposure, and longer treatments were avoided to prevent further heating. The dependence of the data on total UV exposure was not studied in detail, but additional 5 min exposures led to little or no further decrease in the (I MNN)/(N KLL) ratio. Further discussion of radiation-induced change in the (I MNN)/(N KLL) ratio is given in Section 3.4.

3.2. ELS

Fig. 3 shows ELS data for adsorbed 4-chloro- and 4-iodoaniline. Both show the $\pi \rightarrow \pi^*$ excitation of the phenyl ring as the only significant loss feature in the 0–16 eV range. 4-Chloroaniline shows additional weak structure at about 5 and 10 eV. For 4-iodoaniline, the $\pi \rightarrow \pi^*$ peak is broadened to higher energy, suggesting additional loss intensity. In either case, the ELS data indicate adsorption with the phenyl ring intact and the removal of the 3.4 eV GaN surface-state loss feature, as observed [5,6] for other such species. Exposure of the 4-iodoaniline-dosed surface to UV radiation caused a small but reproducible loss of intensity just above the $\pi \rightarrow \pi^*$ peak, suggesting (see below) photolysis of the molecular C–I bond. No similar effect was noted for 4-chloroaniline, for which the $\pi \rightarrow \pi^*$ ELS peak is somewhat narrower than for aniline [5].

The importance of various extraneous factors was assessed using the ELS data and the (I MNN)/(N KLL) peak-height ratio discussed above. To determine the effect of the temperature rise during UV exposure, the sample with adsorbed 4-iodoaniline was heated, in the absence of UV radiation, with a temperature vs. time similar to that during exposure. Little or no effect was seen. Likewise, the (I MNN)/(N KLL) ratio did not change during repeated XPS scans, and the source radiation used in XPS and in UPS (see below) had no discernible effect on the ELS data. Repeated

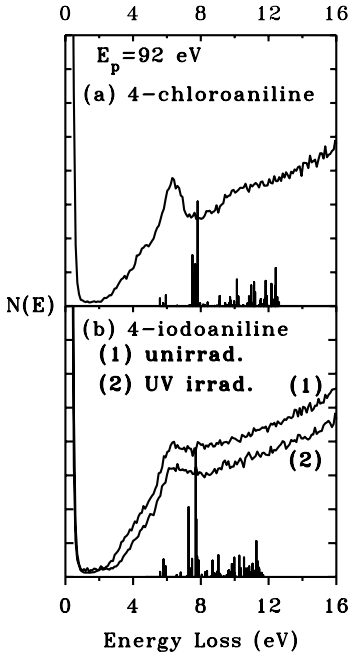

Fig. 3. Surface-sensitive ELS data (92 eV primary beam) for GaN(0 0 0 1) after exposure to (a) 4-chloroaniline and (b) 4-iodoaniline. In (b), the effect of Hg-arc radiation is shown. Relative intensities are quantitative. The instrumental resolution (full-width at half-maximum of the elastic peak) is 0.5 eV. The vertical lines give the results of CIS calculations (up to ~12 eV) of the optical absorption spectra of the free molecules (see text).

ELS scans, which were done using pulse-counting with a primary beam current of ~0.3 μA/cm^2, gave no evidence of electron-induced changes in the adsorbed 4-haloanilines during ELS under the conditions used here.

To examine the ELS data further, ab initio quantum-chemical calculations were performed using *Gaussian98* [26]. The geometries of the free molecules were first optimized using density functional theory (DFT) with the B3LYP functional and 6-31G* basis sets for all atoms except I, for which the LanL2DZ effective core pseudopotential (ECP) was used. Structural data for 4-chloroaniline are available from X-ray crystallography [15,27] and from microwave spectroscopy of the vapor [28], and the computed bond lengths and angles were in good agreement with experiment (within 0.05 Å and 1° respectively). Electronic absorption spectra of the free molecules (up to ~12 eV) were then computed using the configuration interaction singles (CIS) method [29]. Here 6-31$^+$G* basis sets were used for all atoms except I, for which the LanL2DZdp ECP [4] developed by Check et al. [30] was used. This ECP is consistent [30] with the 6-31$^+$G* basis sets used for the lighter atoms which facilitates comparison of results for different molecules.

The CIS results (Fig. 3) overestimate the $\pi \rightarrow \pi^*$ transition energies by ~1.5 eV due to incomplete treatment of electron correlation. No optical data are available for either compound above ~6 eV. However, near-UV data for 4-chloroaniline in various solvents [8,31] show a weak absorption at 4.2 eV and a stronger one at 5.1 eV, in qualitative agreement with the lines at ~5.5–6 eV in the CIS result (Fig. 3a). The ECP used for I is "pseudo-relativistic" [32] but does not include spin–orbit coupling. Hence, all the CIS intensity is in the spin-allowed singlet → singlet transitions and none in the spin-forbidden singlet → triplet excitations. Nevertheless, the computed spectra show additional intensity above the $\pi \rightarrow \pi^*$ band of 4-iodoaniline (in the 8–10 eV range of the CIS result) as observed in ELS. Hence, the broadening of the ELS peak in Fig. 3b may be taken as a "fingerprint" for I bonded to the phenyl ring. Likewise, the UV-induced narrowing of this peak is taken as an indication of the removal of I from at least some of the phenyl rings. A calculation that included spin–orbit coupling would be expected to show even more broadening in the computed 4-iodoaniline spectrum, with intensity distributed between singlet and triplet excited states. Such spin–orbit coupling effects will be much weaker in

[4] The LanL2DZdp ECP was obtained from the Extensible Computational Chemistry Environment Basis Set Database, Version 11/29/01, as developed and distributed by the Molecular Science Computing Facility, Environmental and Molecular Sciences Laboratory which is part of the Pacific Northwest Laboratory, P.O. Box 999, Richland, Washington 99352, USA, and funded by the US Department of Energy. The Pacific Northwest Laboratory is a multi-program laboratory operated by Battelle Memorial Institute for the US Department of Energy under contract DE-AC06-76RLO 1830. Contact David Feller or Karen Schuchardt for further information. The URL is http://www.emsl.pnl.gov:2080/forms/basisform.html.

the case of the lighter Cl atom (i.e., in 4-chloroaniline).

3.3. UPS

3.3.1. Free molecules

We next consider UPS data for the free (gas-phase) molecules. The use of quantum-chemical calculations to analyze the adsorbate UPS (see below) depends on an ability to model the free-molecule spectra and to identify those features that are derived from halogen or NH_2 orbitals. Fig. 4 shows the data [33] together with DFT results. For the molecular structures optimized as above, orbital energies were computed using the B3LYP functional and the same basis sets used for the CIS calculations. For later comparison to adsorbate UPS data, the resulting orbital energy distributions were gaussian-broadened by 1 eV to simulate instrumental and "solid-state" effects. Each density of states (DOS) was shifted in energy to bring the highest occupied molecular orbital (HOMO) into alignment with that of the respective experimental spectrum, at ~8 eV below vacuum (E_V).

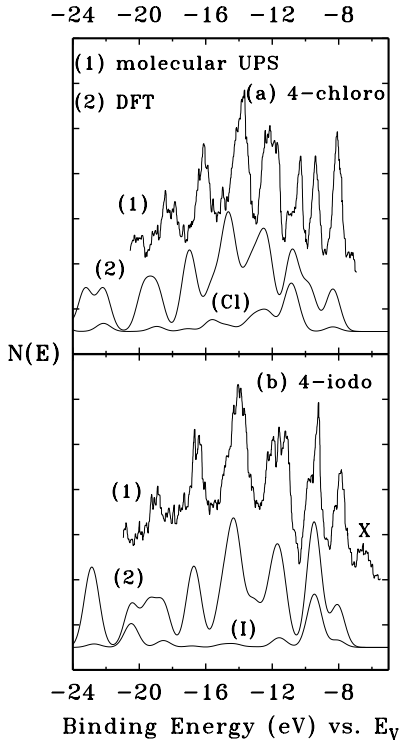

Fig. 4. Comparison of HeII UPS data for gas-phase molecules (Ref. [33], with permission) with DFT results. In either panel, trace (1) gives the data with BE referenced to vacuum, and trace (2) shows the DFT result after alignment at the observed HOMO. Deeper-lying states in the DFT results, below −24 eV, have been truncated. In (b), the feature marked "X" at about −6 eV is apparently an artifact, since it was not assigned in Ref. [33] and not seen in HeI UPS data. The contributions of the respective halogen atoms to the total calculated spectra are shown.

Table 1
Computed atomic subshell photoionization cross-sections (σ, in units of 10^6 barns) for HeI ($h\nu = 21.2$ eV) and HeII ($h\nu = 40.8$ eV) excitation, from Yeh and Lindau [34]. Missing values are inaccessible for HeI

Atomic shell	HeI	HeII
H 1s	1.888	0.2892
C 2s	1.230	1.170
C 2p	6.128	1.875
N 2s		1.086
N 2p	9.688	4.351
Cl 3s		0.4020
Cl 3p	13.84	0.6470
I 5s		0.2169
I 5p	7.985	0.7803

The quantity calculated is a DOS, not an actual spectrum, since the dependence of photoionization cross-section (σ) on orbital composition is neglected. In relation to HeII ($h\nu = 40.8$ eV) UPS data, the results of Yeh and Lindau [34] (Table 1) indicate that the DOS overestimates the intensity of "s-like" orbitals (i.e., those at 20 eV or more below E_V) relative to "p-like" orbitals and also exaggerates the relative intensity of halogen-derived features. The agreement between observed and calculated orbital energies (and even, fortuitously, the DOS relative intensities) is quite good for 4-iodoaniline but less so for 4-chloroaniline. Use of larger basis sets in the orbital energy calculation (6-311^{++}G** for all atoms) gave a 4-chloroaniline DOS virtually identical to that in Fig. 4a(2). Fig. 4 also shows the partial densities of states (PDOS) for the halogen atoms which identify those features receiving significant contributions from halogen orbitals. Contour plots of the various orbitals (not shown) also aid in the assignments.

The halogen character of UPS features at low binding energy (BE) will be useful in the following section and is summarized here. For 4-chloroaniline, the Cl contribution to the DOS peak at −12.5 eV arises from the C–Cl σ-bonding orbital, and the contribution to the DOS peak at −10.8 eV arises from Cl 3p non-bonding orbitals (NBOs). For 4-iodoaniline, the I contributions to the peaks at −11.5 and −9.3 eV arise, respectively, from the C–I σ-bonding orbital and I 5p NBOs. For both molecules, halogen NBOs also make small contributions to the HOMO.

3.3.2. Adsorbed molecules and photoeffects

Figs. 5 and 6 show UPS difference data ($\Delta N(E)$ = adsorbed minus clean) before and after Hg-arc exposure. The results were obtained by scaling and shifting the clean-surface spectrum so as to minimize the intensity of the Ga 3d, at about −19 eV, in the difference. The nearly complete cancellation in $\Delta N(E)$ shows that any change in the Ga 3d is much less than the linewidth. Figs. 5 and 6 also show the computed DOSs, repeated from Fig. 4, together with the NH_2 PDOSs.

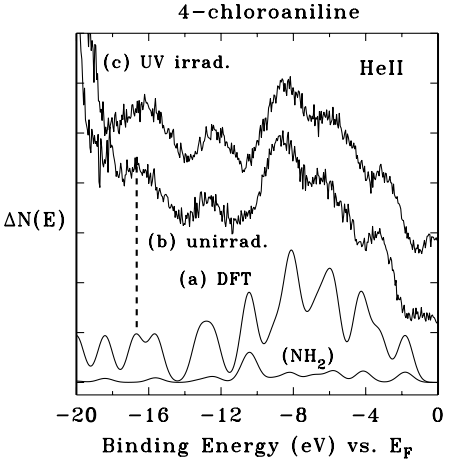

Fig. 5. HeII UPS ($h\nu = 40.8$ eV) data for 4-chloroaniline adsorbed on p-type GaN(0 0 0 1), before and after Hg-arc exposure, compared with the DFT result for the free molecule. Trace (a) shows the DFT result, repeated from Fig. 4a(2). The contribution of the NH_2 group to the calculated free-molecule spectrum is shown. Trace (b) shows the difference spectrum (adsorbed minus clean) before near-UV exposure, and trace (c) shows the difference spectrum after exposure. The BE is referenced to the Fermi level (E_F). The vertical dashed line at about −16.5 eV shows the alignment of the calculated and observed spectra (see text). The rapidly-increasing signal below −19 eV is due to HeI excitation ($h\nu = 21.2$ eV). The instrumental resolution is 0.4 eV, and each data set (clean, adsorbed and UV-exposed) was obtained by averaging two scans.

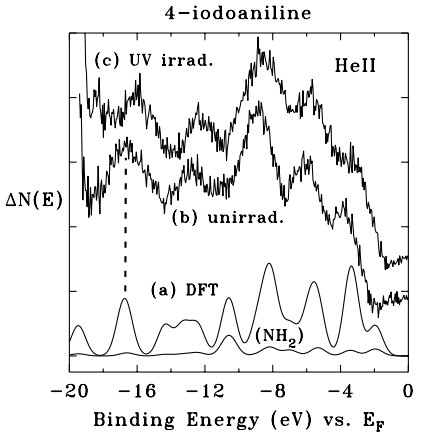

Fig. 6. Similar to Fig. 5 but showing results for 4-iodoaniline.

Alignment of the free-molecule and $\Delta N(E)$ data was done by assuming that deep-valence molecular orbitals (MOs), such as that giving rise to the $\Delta N(E)$ peak at about −16.5 eV for either adsorbate, are unaffected by adsorption other than in undergoing a relaxation shift, ΔE_R, to lower BE relative to E_V. For a non-metallic substrate, $\Delta E_R \approx 1$ eV is a typical value (e.g., Ref. [35]). From the slow-secondary photoelectron threshold (not shown), E_V of the adsorbate-covered p-type GaN surface [5] was located at about 5.8 (5.5) eV above E_F for 4-chloro- (4-iodo-) aniline. This means that the adsorbate peaks at −16.5 eV (vs. E_F) in Figs. 5 and 6 correlate with the free-molecule peaks at −23.2 and −22.8 eV (vs. E_V) in Fig. 4a(2) and b(2), respectively.

With this alignment, the $\Delta N(E)$ data resemble those for aniline [5]. The molecular peaks at about −1.9 and −10.5 eV (Figs. 5a and 6a), which receive

[5] Surface photovoltaic shifts can be significant in UPS and XPS of p-type GaN [36]. Hence, the p-GaN work functions ($E_V - E_F$) given here may be substantially larger than the true (in the dark) values, as would be measured with a Kelvin probe. However, this does not affect the present discussion of adsorbate MO binding energies relative to E_V or to the VBM.

a significant contribution from the NH_2, are essentially absent in $\Delta N(E)$ since bonding occurs via this part of the molecule. The calculated 4-iodoaniline peak at about −14.5 eV (Fig. 6a), which arises largely from I s-like orbitals, is also absent since $\sigma_{5s}(I)$ is relatively small for HeII excitation (cf. Table 1). As was seen for aniline [5], the remaining features in $\Delta N(E)$ are shifted only slightly to higher BE, if at all, relative to those of the free molecule which indicates only a weak effect of adsorption on ring orbitals.

As a final point before discussing radiation effects, the change in electron affinity ($\Delta\chi$) caused by adsorption was obtained from UPS data as described previously [5,6] and found to be negligible (i.e., <0.1 eV) for either species. The n-GaN sample was used here to avoid possible complications due to adsorption-induced changes in the large p-GaN surface photovoltage [36]. These results are in contrast to the case of aniline [5] ($\Delta\chi \approx -0.55$ eV) and indicate a negligible value for the net surface-normal dipole moment in the adsorbed layer.

Irradiation has little effect on the 4-chloroaniline spectrum (Fig. 5) but for 4-iodoaniline (Fig. 6) there is a change in the appearance of features within ~8 eV of E_F. Although HeII excitation reveals a wider range of the spectrum than does HeI ($h\nu = 21.2$ eV), thereby aiding peak assignments, the halogen-derived features are relatively weak (cf. Table 1). The UV-induced changes appear to affect mainly those features derived in part from I atomic orbitals. Hence, to clarify the radiation-induced effects, the experiments in Figs. 5b and c, 6b and c were repeated for HeI excitation and the results shown in Figs. 7 and 8. These reproduce, with a much higher signal/noise ratio, the HeII data in the 0–10 eV range. In separate experiments, involving heating in the absence of UV radiation, it was verified that the effects shown in the HeI data do not result from sample heating (see above) during Hg-arc exposure. Results obtained for exposures using the H_2 discharge source described above were similar to, but weaker than, those in Figs. 7 and 8. Furthermore, the results for n- and p-type GaN were essentially the same.

With the increased relative intensity for I 5p orbitals in HeI vs. HeII, a radiation-induced loss

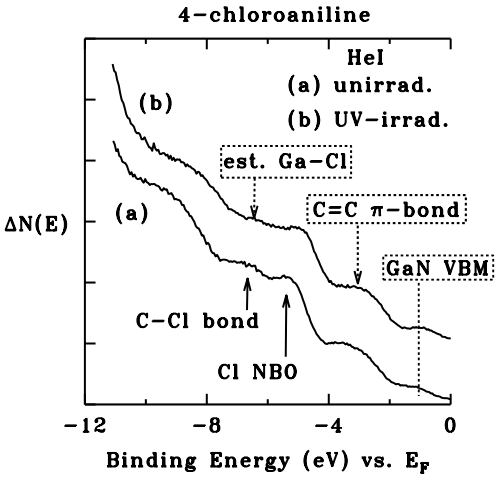

Fig. 7. Similar to Fig. 5b and c but using HeI excitation. Each data set was obtained in a single scan at 0.40 eV resolution. The position of the GaN VBM on the adsorbate-covered surface is indicated. The intensity above the GaN VBM is due to higher-energy satellites in the HeI spectrum and to HeII-excited photoemission features. The increasing intensity toward higher BE results from slow-secondary electron emission. Peaks are labelled which derive a large part of their intensity from C–Cl σ-bonding and Cl NBOs. Also shown is the estimated position of the Ga–Cl bonding orbital, based on data for Cl_2/GaAs(1 1 0) in Ref. [38]. See text for details.

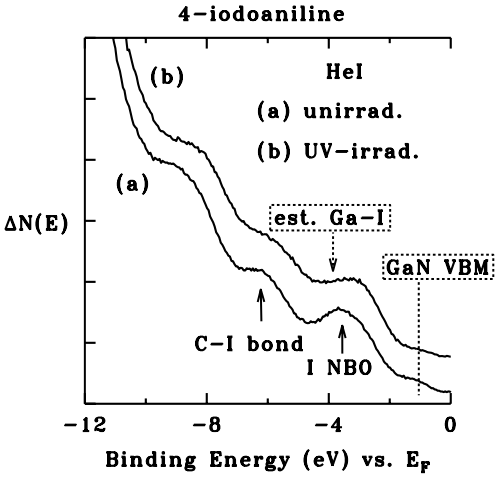

Fig. 8. Similar to Fig. 7a and b but for 4-iodoaniline. Peaks are labelled which derive a large part of their intensity from C–I σ-bonding and I NBOs. Also shown is the estimated position of the Ga–I bonding orbital, based on data for I_2/GaAs(1 1 0) in Ref. [39].

of intensity can now be seen in the C–I σ-bonding orbital (Fig. 8), consistent with photolytic cleaving of the C–I bond. There is possibly a similar, but much weaker, effect for the C–Cl bond in 4-chloroaniline (Fig. 7). The peak at about −9 eV for either adsorbate, which is due largely to ring orbitals, is unaffected by UV exposure. Similarly unaffected is the 4-chloroaniline peak at −3.5 eV which arises from the molecular HOMO-1, a π-bonding orbital involving the 2,3 and 5,6 ring carbons. For 4-iodoaniline, the HOMO-1 is nearly degenerate with the I 5p NBOs at −3.5 eV. For either spectrum, the GaN valence band maximum (VBM) was found [5] to lie at ∼1.1 eV below E_F using the BE vs. E_F of the HeII-excited Ga 3d on the adsorbate-covered surface (not shown) and the known value [37] for the Ga 3d-VBM energy separation.

In Fig. 8 UV radiation causes an apparent filling-in of intensity below the I NBO peak which suggests transfer of I from the adsorbate to the surface in the form of a Ga–I bond. It is unclear whether a similar effect occurs for 4-chloroaniline (Fig. 7). For I_2 adsorption on GaAs(1 1 0), HeI UPS reveals a peak at 2.7 eV below the VBM due to Ga–I bonding orbitals [39]. Fig. 8 shows the location of the corresponding Ga–I orbital on GaN, with the assumption that its position relative to the VBM is the same as for I_2/GaAs(1 1 0). A similar estimate based on data for Cl_2/GaAs(1 1 0) [38] places the Ga–Cl bonding orbital at 5.3 eV below the VBM, as indicated in Fig. 7. In support of the correlation between the UPS data for halogens on GaN(0 0 0 1) and on GaAs(1 1 0) it is noted that the position of the Cl NBO in Fig. 7, ∼4.0 eV below the VBM, agrees with that observed [38] for Cl/GaAs(1 1 0).

3.3.3. Additional experiments

In an effort to verify Ga–Cl or Ga–I bonding following near-UV exposure, the HeII-excited Ga 3d and Mg K$\alpha_{1,2}$-excited Ga $2p_{3/2}$ spectra were examined for evidence of chemically-shifted satellites. Because of the small photoelectron kinetic energies (about 16 and 132 eV, respectively) the surface sensitivities were nearly ideal, and the instrumental resolution was about 0.40 eV (0.75 eV) for the Ga 3d ($2p_{3/2}$) spectrum. The I 3d spectrum (cf. Fig. 2) was also searched for evidence of conversion of C–I to Ga–I bonds, with an instrumental resolution of ∼1.0 eV. Here, photoelectron kinetic energy is not a deciding factor in surface sensitivity because all I is located near the surface. However, no structure was detected in any of these data, possibly due to the large linewidths and small chemical shifts.

Homolytic photodissociation of the C–I bond is expected to leave behind, at least temporarily, a molecular radical species. No new molecular features were observed in UPS after UV irradiation, other than as noted above, which may indicate that the radical either is short-lived or is undetectable against the background of unreacted adsorbates. Experiments were performed in which adsorbed 4-iodoaniline was UV-irradiated (with the Hg-arc) in a background of $\sim 1 \times 10^{-6}$ Torr of either CH_3I or 1,3-butadiene in an effort to promote a reaction with the radical species. No evidence, in the form of a change in ELS or UPS data or an increased C 1s XPS intensity, was observed. This could indicate that the radical formed by C–I dissociation in adsorbed 4-iodoaniline is short-lived or that the attempted reactions are kinetically limited under these low-pressure conditions.

3.4. Model for photodissociation

For 4-iodoaniline there is clear evidence in both ELS (Fig. 3) and HeI UPS (Fig. 8) for photodissociation of the molecular C–I bond. The existence of these radiation-induced effects also implies that the C–I bond is intact in the chemisorbed molecule prior to near-UV exposure. The evidence is less clear for 4-chloroaniline, for which the only indication of possible C–Cl photodissociation is a very subtle change in the HeI UPS (Fig. 7). With the spectroscopic tools at hand, 4-chloroaniline is a more difficult system due to the relatively poor resolution of Cl-derived features in UPS and XPS and to the lack of a fingerprint for C–Cl bonding in ELS. Nevertheless, comparing data for the two adsorbates is useful in interpreting features in the spectra which, in turn, is essential in analyzing the photoeffects. In the following, attention will focus entirely on 4-iodoaniline.

The results suggest that UV radiation dissociates the molecular C–I bond, releasing I which

adsorbs at available Ga sites on the GaN surface not blocked by the aniline fragment. The process is self-limited. It stops when all such sites are filled, and further UV exposure leads to no additional changes. The photochemical changes occur with little or no loss of I from the surface (see below) which argues against desorption of I into vacuum either directly (from C–I bond dissociation) or from Ga–I sites.

It remains to account for the small radiation-induced decrease in the (I MNN)/(N KLL) intensity ratio. An effective attenuation length of 12.3 Å, for 500 eV I MNN electrons (cf. Fig. 2) in a layer of elemental carbon (graphite), was obtained from a standard database [6] [40] which includes the effects of elastic scattering of the Auger electrons. With this result and the XAES collection angle of 42°, an effective C layer thickness of only ~1.8 Å (vs. a C covalent radius of 0.77 Å) would account for the ~18% loss of I MNN intensity seen following near-UV exposure. Thus, this small effect can reasonably be ascribed to partial shadowing of Ga–I sites by the adsorbed phenyl rings. A more quantitative discussion is difficult without a detailed structural model for the surface layer.

The present photoeffects are essentially independent of substrate carrier type which argues against a substrate-mediated process [3] involving transfer of photoexcited electrons from the GaN CB into the adsorbate LUMO or of photoexcited holes from the GaN VB into the adsorbate HOMO. The UPS data (Fig. 8) show that the adsorbate HOMO is centered at ~2 eV below the GaN VBM, making the transfer of thermalized holes from the VBM to the adsorbate energetically unfavorable.

A similar conclusion is reached concerning the transfer of thermalized electrons from the CBM to the adsorbate LUMO. Since, as noted above, $\Delta\chi \approx 0$, the energy difference between E_V and the CBM is essentially unaffected by 4-iodoaniline. A measured electron affinity (EA) for the free 4-iodoaniline molecule is not available, but Table 2 gives computed values for relevant species. As a check, the calculated EA for aniline agrees well with experiment. Following Wu et al. [43], the vertical EA from Table 2, the GaN EA of +3.2 eV and the relaxation shift of $\Delta E_R \approx 1$ eV (discussed above) combine to center the 4-iodoaniline LUMO at ~2.6 eV above the GaN CBM.

Table 2
Computed electron affinities (eV) for free molecules[a]

Molecule	Vertical[b]	Adiabatic[c]
Aniline	−1.10	−1.07[d]
4-Chloroaniline	−0.885	−0.030
4-Iodoaniline	−0.369	+0.628

[a] Positive (negative) values mean that the anion is more (less) stable than the neutral molecule. All energy calculations used the same basis sets as for the CIS treatment (see text).

[b] Difference in energy between the anion and the neutral molecule with the anion geometry "frozen" in the optimized configuration of the ground-state neutral (cf. Ref. [41]).

[c] Difference in energy between the anion and the neutral molecule with both geometries optimized. The anion geometries were optimized using the UB3LYP functional with the same basis sets as used for optimizing the geometries of the neutral species (see text). Adiabatic values include the difference in zero-point vibrational energy between anion and neutral (cf. Ref. [41]).

[d] The corresponding experimental value is −1.13 eV (Ref. [42]).

Excitation of electrons from the VBM into the adsorbate LUMO has been observed [44] in the UV photodissociation of CH_3Br on GaAs(1 1 0). In the present case, the large downward band bending on p-GaN(0 0 0 1) (~1.0 eV under illumination, Ref. [36]) would act to accelerate such a process in comparison to n-GaN, with an upward band bending of ~0.8 eV. Such a difference was not observed here.

The absence of an effect due to photoexcited carriers suggests that direct excitation of the adsorbed 4-iodoaniline leads to C–I cleaving. The CIS results provide an indication of which MOs are the initial states for photochemical excitation. The UPS data show that the HOMO of the free molecule is strongly perturbed by chemisorption. Neglecting this MO, excitations up to and including the strong ELS peak in 4-chloroaniline involve primarily the uppermost ring π orbital (4a″ in the notation of Ref. [33]) which consists of π bonds between the 2,3 and 5,6 carbons. On the

[6] See http://www.nist.gov/srd/nist82.htm for information on obtaining this database.

other hand, for 4-iodoaniline, transitions in this part of the spectrum receive significant contributions from both the 4a″ π and I NBOs. This is true for both the singlet excited states shown in Fig. 3 and the triplet states in the same energy range which should be accessible via spin–orbit coupling on the I atom, as discussed above. The final states in these transition have significant C–I σ^* antibonding character; hence, the photodissociation process can be described as an $n \rightarrow \sigma^*$ transition localized on the C–I bond.

4. Summary and conclusions

The adsorption of 4-chloro- and 4-iodoaniline on the GaN(0 0 0 1)-(1 × 1) surface, and the effects of subsequent exposure to UV radiation, have been studied using primarily UV photoemission and electron energy loss spectroscopies, supported by ab initio quantum-chemical modeling. The results are as follows:

(1) Both 4-haloanilines adsorb via the molecular NH_2 group, with the phenyl ring intact, as does aniline itself. Like aniline, both are very reactive with the clean GaN(0 0 0 1)-(1 × 1) surface, requiring only a small dose to achieve a saturation coverage.
(2) Iodoaniline is photochemically active as an adsorbate on GaN, as expected from its suggested behavior in non-polar solvents. Near-UV radiation promotes dissociation of the molecular C–I bond, leading to the transfer of I to available sites on the GaN surface. The molecular C–I bond is intact prior to exposure, as suggested by the changes in ELS and UPS data seen to result from UV exposure.
(3) The photochemical activity of 4-chloroaniline adsorbed on GaN is uncertain, but it appears to be relatively inert under the present conditions.
(4) Photochemical dissociation of the C–I bond appears to proceed by direct excitation of the molecule (specifically the $n \rightarrow \sigma^*$ transition) rather than through a substrate mediated process involving transfer of excited carriers between adsorbate and substrate.

Further work is needed to establish the 4-iodoaniline chemistry described here as a viable route for surface photosynthesis of functional structures. One issue is whether the self-limiting nature of the photodissociation can be circumvented, e.g., by annealing at some appropriate temperature during near-UV exposure to promote desorption from Ga–I sites. A study of temperature programmed desorption before and after near-UV exposure is essential here. Another issue concerns identifying the electronic structure of the chemisorbed phenylamine fragment remaining after C–I bond dissociation since this is the desired site for photosynthetic reaction.

Experimental detection of Ga–I bonds after UV exposure would be helpful in refining the proposed model. Vibrational spectroscopy, by either IR or ELS methods, would be difficult for the Ga–I bond-stretching mode of a small coverage of I on a partially ionic substrate such as GaN. A direct and practicable method for detecting Ga–I bonds would be through the use of photon stimulated desorption spectroscopy (e.g., Ref. [45]) to correlate peaks in I^+ ion yield with excitation of Ga core levels.

Note added in proof

A recent study [46] of the photodissociation of iodobenzene, C_6H_5I, has shown the importance of $n \rightarrow \sigma^*$ excitation in breaking the C–I bond in this system.

Acknowledgements

This work was supported by the Office of Naval Research and also in part by a grant of computer time from the DOD High Performance Computing Modernization Program at the ASC-MSRC, Wright-Patterson AFB. Helpful communications with A. Albini, J.B. Foresman, G. Grabner, E.I. von Nagy-Felsobuki and J.A. Yarmoff on various aspects of the work are gratefully acknowledged. J.P. Long and J.N. Russell Jr., are also thanked for providing equipment, materials and advice.

References

[1] R.A. Wolkow, Annu. Rev. Phys. Chem. 50 (1999) 413.
[2] R.J. Hamers, S.K. Coulter, M.D. Ellison, J.S. Hovis, D.F. Padowitz, M.P. Schwartz, C.M. Greenlief, J.N. Russell Jr., Acc. Chem. Res. 33 (2000) 617.
[3] W. Cai, Z. Lin, T. Strother, L.M. Smith, R.J. Hamers, J. Phys. Chem. B 106 (2002) 2656.
[4] G. Ashkenasy, D. Cahen, R. Cohen, A. Shanzer, A. Vilan, Acc. Chem. Res. 35 (2002) 121.
[5] V.M. Bermudez, Surf. Sci. 499 (2002) 109.
[6] V.M. Bermudez, Surf. Sci. 499 (2002) 124.
[7] A. Vilan, A. Shanzer, D. Cahen, Nature 404 (2000) 166.
[8] K. Othmen, P. Boule, B. Szczepanik, K. Rotkiewicz, G. Grabner, J. Phys. Chem. A 104 (2000) 9525.
[9] B. Guizzardi, M. Mella, M. Fagnoni, M. Freccero, A. Albini, J. Org. Chem. 66 (2001) 6353.
[10] M. Mella, P. Coppo, B. Guizzardi, M. Fagnoni, M. Freccero, A. Albini, J. Org. Chem. 66 (2001) 6344.
[11] P. Coppo, M. Fagnoni, A. Albini, Tetrahedron Lett. 42 (2001) 4271.
[12] B. Szczepanik, T. Latowski, Pol. J. Chem. 71 (1997) 807.
[13] A. Albini, Department of Organic Chemistry, University of Pavia, private communication.
[14] V. Piacente, P. Scardala, D. Ferro, R. Gigli, J. Chem. Eng. Data 30 (1985) 372.
[15] J.H. Palm, Acta Cryst. 21 (1966) 473.
[16] Integrated Spectral Data Base System for Organic Compounds (SDBS) <http://www.aist.go.jp/RIODB/SDBS/menu-e.html>.
[17] C.T. Campbell, S.M. Valone, J. Vac. Sci. Technol. A 3 (1985) 408.
[18] J.T. Yates Jr., Experimental Innovations in Surface Science, Springer, New York, 1997 (Chapter VI).
[19] The Book of Photon Tools, Oriel Corp., Stratford, CT, USA (1999).
[20] Y. Tanaka, J. Opt. Soc. Am. 45 (1955) 710.
[21] J.A.R. Samson, Techniques of Vacuum Ultraviolet Spectroscopy, Pied Publications, Lincoln, NE, USA, 1967 (Chapter 5).
[22] W.F. Krolikowski, W.E. Spicer, Phys. Rev. B 1 (1970) 478.
[23] E.D. Palik, Handbook of Optical Constants, Academic, Orlando, 1985.
[24] H. Henneken, F. Scholze, G. Ulm, J. Appl. Phys. 87 (2000) 257.
[25] H. Ebel, M.F. Ebel, H. Krocza, Surf. Interface Anal. 12 (1988) 137.
[26] Gaussian98 (Revision A.11), M.J. Frisch, G.W. Trucks, H.B. Schlegel, G.E. Scuseria, M.A. Robb, J.R. Cheeseman, V.G. Zakrzewski, J.A. Montgomery Jr., R.E. Stratmann, J.C. Burant, S. Dapprich, J.M. Millam, A.D. Daniels, K.N. Kudin, M.C. Strain, O. Farkas, J. Tomasi, V. Barone, M. Cossi, R. Cammi, B. Mennucci, C. Pomelli, C. Adamo, S. Clifford, J. Ochterski, G.A. Petersson, P.Y. Ayala, Q. Cui, K. Morokuma, P. Salvador, J.J. Dannenberg, D.K. Malick, A.D. Rabuck, K. Raghavachari, J.B. Foresman, J. Cioslowski, J.V. Ortiz, A.G. Baboul, B.B. Stefanov, G. Liu, A. Liashenko, P. Piskorz, I. Komaromi, R. Gomperts, R.L. Martin, D.J. Fox, T. Keith, M.A. Al-Laham, C.Y. Peng, A. Nanayakkara, M. Challacombe, P. M.W. Gill, B. Johnson, W. Chen, M.W. Wong, J.L. Andres, C. Gonzalez, M. Head-Gordon, E.S. Replogle, J.A. Pople, Gaussian, Inc., Pittsburgh, PA, 2001.
[27] V.R. Sarma, Indian J. Pure Appl. Phys. 4 (1966) 226.
[28] A. Nonat, A. Bouchy, G. Roussy, J. Mol. Struct. 116 (1984) 227.
[29] J.B. Foresman, M. Head-Gordon, J.A. Pople, M.J. Frisch, J. Phys. Chem. 96 (1992) 135.
[30] C.E. Check, T.O. Faust, J.M. Bailey, B.J. Wright, T.M. Gilbert, L.S. Sunderlin, J. Phys. Chem. A 105 (2001) 8111.
[31] I. Iweibo, R.A. Oderinde, J.A. Faniran, Spectrochim. Acta 38A (1982) 1.
[32] P.J. Hay, W.R. Wadt, J. Chem. Phys. 82 (1985) 299.
[33] J.L.D. Sky, E.I. von Nagy-Felsobuki, J. Mol. Struct. 475 (1999) 241.
[34] J.J. Yeh, I. Lindau, Atom. Data Nucl. Data Tables 32 (1985) 1.
[35] K.Y. Yu, J.C. McMenamin, W.E. Spicer, Surf. Sci. 50 (1975) 149.
[36] J.P. Long, V.M. Bermudez, Phys. Rev. B (Rapid Commun.) 66 (2002), in press.
[37] J.R. Waldrop, R.W. Grant, Appl. Phys. Lett. 68 (1996) 2879.
[38] D. Troost, H.J. Clemens, L. Koenders, W. Mönch, Surf. Sci. 286 (1993) 97.
[39] D. Troost, L. Koenders, W. Mönch, Appl. Surf. Sci. 65/66 (1993) 619.
[40] C.J. Powell, A. Jablonski, NIST Electron Effective-Attenuation-Length Database (NIST Standard Reference Database 82), US National Institute of Standards and Technology, Gaithersburg, MD, 2001.
[41] J.C. Rienstra-Kiracofe, G.S. Tschumper, H.F. Schaefer III, S. Nandi, G.B. Ellison, Chem. Rev. 102 (2002) 231.
[42] K.D. Jordan, J.A. Michejda, P.D. Burrow, J. Am. Chem. Soc. 98 (1976) 7189.
[43] C.I. Wu, Y. Hirose, H. Sirringhaus, A. Kahn, Chem. Phys. Lett. 272 (1997) 43.
[44] N. Camillone III, K.A. Khan, P.J. Lasky, L. Wu, J.E. Moryl, R.M. Osgood Jr., J. Chem. Phys. 109 (1998) 8045.
[45] P.R. Varekamp, W.C. Simpson, D.K. Shuh, T.D. Durbin, V. Chakarian, J.A. Yarmoff, Phys. Rev. B 50 (1994) 14267.
[46] K. Kavita, P.K. Das, J. Chem. Phys. 117 (2002) 2038.